

Comparison of Recursive Estimation Techniques for Position Tracking Radioactive Sources

Kenneth R. Muske

Department of Chemical Engineering, Villanova University, Villanova, PA 19085-1681

James W. Howse

Computational Science Methods, Los Alamos National Laboratory, Los Alamos, NM 87545

Abstract

This paper compares the performance of recursive state estimation techniques for tracking the physical location of a radioactive source based on radiation measurements obtained from a series of detectors at fixed locations. Specifically, the first order, iterated, and a second order extended Kalman filter performance is compared to nonlinear least squares estimation. The results of this study indicate that least squares estimation significantly outperforms the extended Kalman filter implementations in this application due to the nature of the model nonlinearities.

1. Introduction

The position tracking system consists of a single radioactive source of known strength and initial position within a room containing four radiation detectors. The radiation detectors are located at fixed positions on each wall of the room and provide discrete count rate measurements at a one second sample period. The count rate for a given sensor represents the total number of gamma-energy photons detected by that sensor over the one second sample period. We wish to track the position of the source in real time as it is moved within the room based on the radiation detector measurements. The estimate of the source location is based on a nonlinear model for each sensor that relates the detector count rate to location.

2. Dynamic Model

The state of the system, $\mathbf{s} = [x \ y \ z \ \mathcal{B}]^T$, consists of the x - y - z coordinates of the position of the source within the room and the background radiation, \mathcal{B} , which also changes. Since the background radiation does not vary significantly, the source is normally stationary, and there is no prescribed trajectory or relationship between the displacement in each of the coordinate directions when it is moved, we choose to model the state dynamics as a random walk process in which $\boldsymbol{\omega}$ is an independent, normally distributed disturbance.

$$\dot{\mathbf{s}} = \mathbf{0} + \boldsymbol{\omega} \quad (1)$$

The system measurements consist of the count rates, $\boldsymbol{\mathcal{M}} = [\mathcal{M}_1 \ \mathcal{M}_2 \ \mathcal{M}_3 \ \mathcal{M}_4]^T$, from the four radiation detectors in which the subscript indicates the detector. The count rate measured by the i th detector can be determined from the source strength, detector properties, view factor, and the current state of the system from the following relationship [1]

$$\mathcal{M}_i = \frac{\Omega_i \mathcal{S} \epsilon_i \mathcal{F}_i + \mathcal{B}}{1 + \tau_i \Omega_i \mathcal{S} \epsilon_i \mathcal{F}_i} + \nu_i, \quad i = 1, \dots, 4 \quad (2)$$

in which \mathcal{S} is the source strength in counts per second, $\epsilon_i = 0.1$ is the detector efficiency, $\tau_i = 3.3$ nsec is the detector dead time, \mathcal{F}_i is the product of all correction factors such as absorption and backscattering which is assumed to be unity for each detector in this work, \mathcal{B} is the number of counts per second which constitutes the background radiation, and $\boldsymbol{\nu}$ is an independent, Poisson distributed measurement noise vector.

The view factor for each detector, Ω_i , is the ratio of the number of particles which actually enter the detector to the total number of particles emitted by the source. Assuming a point source located at coordinates (u, v, w) relative to the detector and a detector of width \mathcal{W} and height \mathcal{H} , the quantity Ω_i is modeled as the solid angle subtended by the detector [2]

$$\begin{aligned} \Omega_i(u_i, v_i, w_i) = & \tan^{-1} \left(\frac{u_i v_i}{|w_i| \sqrt{u_i^2 + v_i^2 + w_i^2}} \right) \\ & - \tan^{-1} \left(\frac{(u_i - \mathcal{W}) v_i}{|w_i| \sqrt{(u_i - \mathcal{W})^2 + v_i^2 + w_i^2}} \right) \\ & - \tan^{-1} \left(\frac{u_i (v_i - \mathcal{H})}{|w_i| \sqrt{u_i^2 + (v_i - \mathcal{H})^2 + w_i^2}} \right) \\ & + \tan^{-1} \left(\frac{(u_i - \mathcal{W}) (v_i - \mathcal{H})}{|w_i| \sqrt{(u_i - \mathcal{W})^2 + (v_i - \mathcal{H})^2 + w_i^2}} \right) \end{aligned} \quad (3)$$

in which $\mathcal{H} = 0.253$ m and $\mathcal{W} = 0.914$ m for the detectors used in this study. The expression in Eq. 3 is based on a detector-centered coordinate system. Since there are four detectors in this study, it

is not possible to choose a coordinate system that is centered at each detector. Therefore, we choose a room-centered coordinate system to describe the source location and determine a coordinate transformation from room-centered to detector-centered coordinates for each detector. The required transformation, which converts room-centered coordinates, (x, y, z) , to detector-centered coordinates, (u_i, v_i, w_i) , for the i th detector, is linear and can be expressed as

$$\begin{pmatrix} u_i \\ v_i \\ w_i \end{pmatrix} = \begin{pmatrix} \cos \mathcal{A}_i & 0 & \sin \mathcal{A}_i & \mathcal{T}_{x,i} \cos \mathcal{A}_i + \mathcal{T}_{z,i} \sin \mathcal{A}_i \\ 0 & 1 & 0 & \mathcal{T}_{y,i} \\ -\sin \mathcal{A}_i & 0 & \cos \mathcal{A}_i & \mathcal{T}_{z,i} \cos \mathcal{A}_i - \mathcal{T}_{x,i} \sin \mathcal{A}_i \end{pmatrix} \begin{pmatrix} x \\ y \\ z \\ 1 \end{pmatrix} \quad (4)$$

in which $\mathcal{T}_{x,i}$, $\mathcal{T}_{y,i}$, and $\mathcal{T}_{z,i}$ are the translations along the room centered x , y , and z directions, respectively, and \mathcal{A}_i is the rotation angle around the v -axis for the i th detector. The source strength and background radiation are invariant under this transformation.

3. Extended Kalman Filters

Extended Kalman filters compute a state estimate at each sampling period by the application of linear Kalman filtering on a linearized model of the nonlinear system around the current state estimate. For the tracking system model presented in Section 2, only the sensor model in Eq. 2 is nonlinear. A linear approximation of this sensor model for use in the extended Kalman filter can be developed using the first order terms of a Taylor series expansion

$$\tilde{\mathcal{M}}(\mathbf{s} + \mathbf{d}) = \mathcal{M}(\mathbf{s}) + \mathcal{G}\mathbf{d} \quad (5)$$

in which $\mathcal{M}(\mathbf{s})$ is the sensor function evaluated at the state \mathbf{s} and \mathcal{G} is the Jacobian matrix of the sensor model function evaluated at the state \mathbf{s} .

$$\mathcal{G} = \begin{pmatrix} \frac{\partial \mathcal{M}_1}{\partial x} & \frac{\partial \mathcal{M}_1}{\partial y} & \frac{\partial \mathcal{M}_1}{\partial z} & \frac{\partial \mathcal{M}_1}{\partial \mathcal{B}} \\ \vdots & \vdots & \vdots & \vdots \\ \frac{\partial \mathcal{M}_4}{\partial x} & \frac{\partial \mathcal{M}_4}{\partial y} & \frac{\partial \mathcal{M}_4}{\partial z} & \frac{\partial \mathcal{M}_4}{\partial \mathcal{B}} \end{pmatrix} \quad (6)$$

$$\begin{aligned} \frac{\partial \mathcal{M}_i}{\partial x} &= \frac{\partial \mathcal{M}_i}{\partial \Omega_i} \left(\frac{\partial \Omega_i}{\partial u_i} \frac{\partial u_i}{\partial x} + \frac{\partial \Omega_i}{\partial v_i} \frac{\partial v_i}{\partial x} + \frac{\partial \Omega_i}{\partial w_i} \frac{\partial w_i}{\partial x} \right) \\ \frac{\partial \mathcal{M}_i}{\partial y} &= \frac{\partial \mathcal{M}_i}{\partial \Omega_i} \left(\frac{\partial \Omega_i}{\partial u_i} \frac{\partial u_i}{\partial y} + \frac{\partial \Omega_i}{\partial v_i} \frac{\partial v_i}{\partial y} + \frac{\partial \Omega_i}{\partial w_i} \frac{\partial w_i}{\partial y} \right) \\ \frac{\partial \mathcal{M}_i}{\partial z} &= \frac{\partial \mathcal{M}_i}{\partial \Omega_i} \left(\frac{\partial \Omega_i}{\partial u_i} \frac{\partial u_i}{\partial z} + \frac{\partial \Omega_i}{\partial v_i} \frac{\partial v_i}{\partial z} + \frac{\partial \Omega_i}{\partial w_i} \frac{\partial w_i}{\partial z} \right) \end{aligned}$$

3.1. First Order Filter

The first order filter uses the approximate sensor model in Eq. 5, linearized about the current state estimate, to construct a time-varying Kalman filter at

each sampling period [3]. The estimate of the state at sample time k given sensor measurements up to time k , $\hat{\mathbf{s}}_{k|k}$, is computed as follows

$$\hat{\mathbf{s}}_{k|k} = \hat{\mathbf{s}}_{k|k-1} + \mathbf{d}_k \quad (7)$$

$$\mathbf{d}_k = \mathbf{L}_k (\mathcal{D}_k - \mathcal{M}_{k|k-1}) \quad (8)$$

$$\hat{\mathbf{s}}_{0|0} = [x_o \ y_o \ z_o \ \mathcal{B}_o]^T \quad (9)$$

in which \mathcal{D}_k is the sensor measurement vector at sample time k , $\mathcal{M}_{k|k-1}$ is the sensor model in Eqs. 2–4 evaluated at the state estimate $\mathbf{s}_{k|k-1}$, and $\mathbf{s}_{0|0}$ is the known initial state. The time-varying linear Kalman filter gain at sample time k , \mathbf{L}_k , is determined by

$$\mathbf{L}_k = \mathbf{P}_{k|k-1} \mathcal{G}_{k|k-1}^T (\mathcal{G}_{k|k-1} \mathbf{P}_{k|k-1} \mathcal{G}_{k|k-1}^T + \mathbf{R})^{-1} \quad (10)$$

in which $\mathcal{G}_{k|k-1}$ is the Jacobian matrix in Eq. 6 evaluated at the state estimate $\mathbf{s}_{k|k-1}$ and $\mathbf{P}_{k|k-1}$ is the estimated state covariance matrix. The estimated covariance of the state is updated at each sample time due to the contribution of the discrete measurement.

$$\mathbf{P}_{k|k} = (\mathbf{I} - \mathbf{L}_k \mathcal{G}_{k|k-1}) \mathbf{P}_{k|k-1} \quad (11)$$

The estimated state and state covariance matrix are updated between sampling times based on the linear state dynamic model presented in Eq. 1.

$$\hat{\mathbf{s}}_{k+1|k} = \hat{\mathbf{s}}_{k|k}, \quad \mathbf{P}_{k+1|k} = \mathbf{P}_{k|k} + \mathbf{Q} \quad (12)$$

The tuning parameters for the filter are the state and measurement noise covariance matrices. Since the radiation detector measurement noise is Poisson distributed, the measurement covariance used for the filter is a diagonal matrix in which each diagonal entry is determined from the model predicted count rate at the current estimate of the state scaled by the squared dispersion. The state disturbance covariance matrix is a diagonal matrix with the variance of the background radiation scaled by a constant value.

$$\mathbf{R} = \text{diag}(\gamma^2 \mathcal{M}_{k|k-1}), \quad \mathbf{Q} = \text{diag}([1, 1, 1, \alpha]) \quad (13)$$

Figures 1 and 2 present the x -direction and y -direction tracking errors for the first order extended Kalman filter applied to a test data set. The values $\gamma = 10$ and $\alpha = 0.01$ were used to obtain these results. Larger values of γ result in poorer tracking performance while smaller values result in excessive variation of the estimated position. For values of $\gamma < 7$, the extended Kalman filter becomes unstable. Larger values of α result in an unreasonable increase in the estimated background radiation. As shown in these figures, the filter is unable to adequately track the source and places it outside of the room for a significant period during the test. The application of position constraints, by clipping state estimates that are outside of the room at each sampling period, does prevent physically unrealistic estimates but does not improve the prediction error significantly.

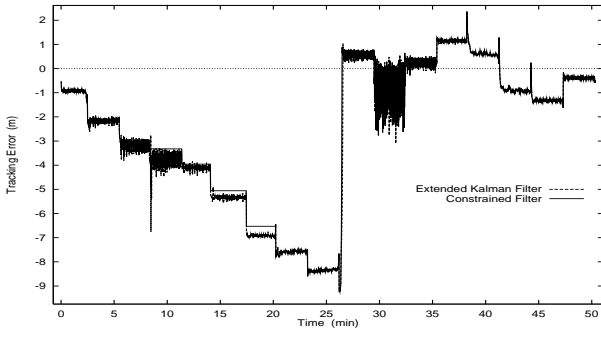


Figure 1: First order filter x -direction tracking error.

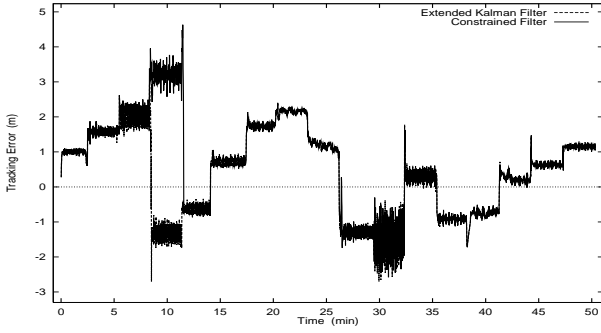


Figure 2: First order filter y -direction tracking error.

3.2. Iterative First Order Filter

Iterative extended Kalman filters attempt to reduce the estimation error by improving the approximation to the nonlinear system that is used in the determination of the filtered state. These schemes linearize the system model about an updated state estimate at each iteration. An iterative scheme used to compensate for nonlinearity in the measurement function is to repeat the calculation of $\hat{s}_{k|k}$ in Eq. 7 [4]. Letting $\hat{s}_{k|k}(i)$ represent the i th iterate of the filtered state estimate, the next iteration is determined as follows

$$\hat{s}_{k|k}(i+1) = \hat{s}_{k|k-1} + d_k(i) \quad (14)$$

$$d_k(i) = L_k(i) (\mathcal{D}_k - \mathcal{M}_{k|k}(i) - \mathcal{G}_{k|k}(i) (\hat{s}_{k|k-1} - \hat{s}_{k|k}(i))) \quad (15)$$

$$\hat{s}_{k|k}(0) = \hat{s}_{k|k-1} \quad (16)$$

in which the filter gain, $L_k(i)$, and the Jacobian of the sensor model function, $\mathcal{G}_{k|k}(i)$, are recomputed at each iteration based on the current iterate of the filtered state. The iteration is repeated until there is no significant difference between the iterated filtered states. The estimated state covariance is then updated in the same manner as Eq. 11 using the converged filter gain and sensor model function Jacobian. The estimated state and covariance are propagated between sampling times in the same manner as the first order filter as shown in Eq. 12.

The iterative first order filter x -direction and y -direction tracking errors are shown in Figures 3 and 4. Values of $\gamma = 10$ and $\alpha = 0.01$ were used to obtain these results with a maximum of ten iterations allowed to get within a 0.1 m tolerance for the 2-norm of the difference between successive iterates. An average of 9 iterations were required for the unconstrained filter and 8 iterations for the constrained filter. In both cases, however, most of the estimates either converged within two to three iterations or did not converge within the iteration limit. Increasing the iteration limit does not result in either convergence or improved estimates. Successive linearization of the sensor model function does not significantly improve the tracking error with almost an order of magnitude increase in computational effort. The incorporation of constraints also decreases the average x -direction tracking performance for the iterated filter.

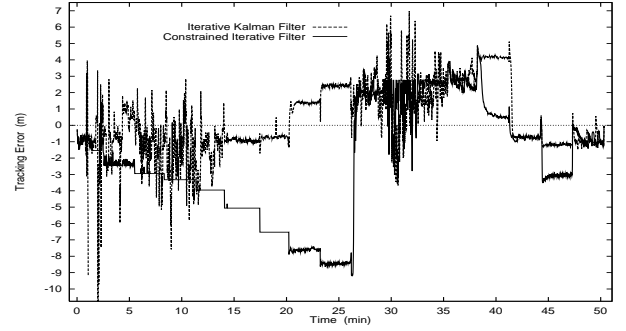


Figure 3: Iterative filter x -direction tracking error.

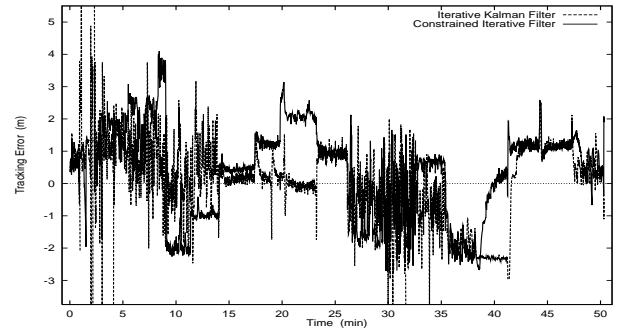


Figure 4: Iterative filter y -direction tracking error.

3.3. Second Order Filter

The second order filter utilizes a second order approximation to the sensor model about the current state estimate. The filter applied in this work is that presented in [5] and referred to as a *modified Gaussian second order filter* in [4].

$$d_k = L_k (\mathcal{D}_k - \mathcal{M}_{k|k-1} - \Pi_k) \quad (17)$$

$$L_k = P_{k|k-1} \mathcal{G}_k^T (\mathcal{G}_k P_{k|k-1} \mathcal{G}_k^T + R + \Gamma_k)^{-1} \quad (18)$$

The terms $\mathbf{\Pi}_k$ in the state estimate update and $\mathbf{\Gamma}_k$ in the filter gain update result from the contribution of the second order terms in the approximation [5]

$$\mathbf{\Pi}_k = \frac{1}{2} \sum_{j=1}^4 e^j \text{tr} \left[\mathbf{G}_k^j \mathbf{P}_{k|k-1} \right] \quad (19)$$

$$\mathbf{\Gamma}_k = \frac{1}{2} \sum_{i=1}^4 \sum_{j=1}^4 e^j e^{iT} \text{tr} \left[\mathbf{G}_k^i \mathbf{P}_{k|k-1} \mathbf{G}_k^j \mathbf{P}_{k|k-1} \right] \quad (20)$$

$$\mathbf{G}_k^i = \left. \frac{\partial^2 \mathcal{M}_i}{\partial \mathbf{s}^2} \right|_{\mathbf{s}=\mathbf{s}_k}, \quad e^i = [0, \dots, \underbrace{1}_{i\text{th location}}, \dots, 0]^T \quad (21)$$

in which \mathbf{G}_k^i is the Hessian matrix of the sensor model of the i th state evaluated at the current state estimate.

$$\mathbf{G}^i = \begin{pmatrix} \frac{\partial^2 \mathcal{M}_i}{\partial x^2} & \frac{\partial^2 \mathcal{M}_i}{\partial x \partial y} & \frac{\partial^2 \mathcal{M}_i}{\partial x \partial z} & \frac{\partial^2 \mathcal{M}_i}{\partial x \partial \mathcal{B}} \\ \vdots & \vdots & \vdots & \vdots \\ \frac{\partial^2 \mathcal{M}_i}{\partial \mathcal{B} \partial x} & \frac{\partial^2 \mathcal{M}_i}{\partial \mathcal{B} \partial y} & \frac{\partial^2 \mathcal{M}_i}{\partial \mathcal{B} \partial z} & \frac{\partial^2 \mathcal{M}_i}{\partial \mathcal{B}^2} \end{pmatrix} \quad (22)$$

Since the state dynamics are linear, the state estimate and state covariance matrix are updated in the same manner as the first order filter using Eq. 12.

Figures 5 and 6 present the x -direction and y -direction tracking errors for the second order filter with $\gamma = 10$ and $\alpha = 0.01$. There is a modest improvement in the tracking error using the second order filter, however, the computational requirements increase by a factor of four over the first order filter. Note that the application of position constraints leads to a significant decrease in the average x -direction tracking performance similar to the iterative filter.

4. Nonlinear Least Squares Estimator

A least squares estimator that explicitly considers sensor noise and position constraints is now considered [6]. At each sample time, the optimal estimated change in the state, \mathbf{d}_k , is determined from the solution to the following nonlinear optimization problem

$$\mathbf{d}_k^* = \arg \min_{\mathbf{d}_k} \left(\sum_{i=1}^4 \mathcal{W}_i^m \left(\mathcal{D}_i - \mathcal{M}_i(\hat{\mathbf{s}}_{k|k-1} + \mathbf{d}_k) \right)^2 + \sum_{j=1}^4 \mathcal{W}_j^d d_j^2(k) \right) \quad (23)$$

Subject to:

$$\mathcal{L}_j \leq \hat{s}_j(k | k-1) + d_j(k) \leq \mathcal{U}_j, \quad j = 1, \dots, 4$$

in which \mathcal{W}_i^m are the model prediction error weights, \mathcal{W}_j^d are the weights for the change from the previous state estimate, \mathcal{L}_j are the minimum position constraints, and \mathcal{U}_j are the maximum position constraints. We select \mathcal{W}_i^m as the diagonal entries of the matrix \mathbf{Q}^{-1} and \mathcal{W}_j^d as the diagonal entries of the matrix \mathbf{R}^{-1} as defined in Eq. 13.

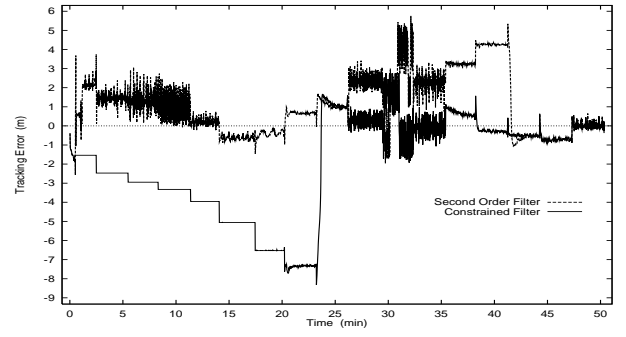


Figure 5: Second order filter x -direction tracking error.

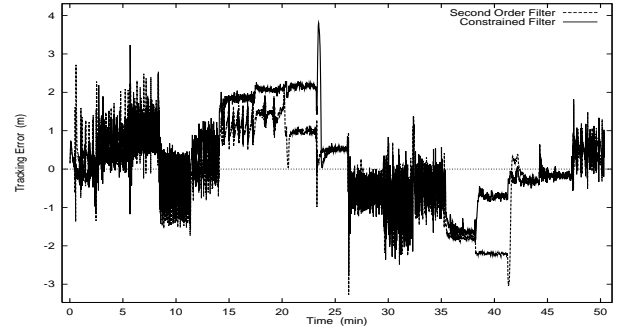


Figure 6: Second order filter y -direction tracking error.

The optimization problem posed in Eq. 23 is solved using a feasible sequential quadratic programming approach [7] in which the solution was generally obtained within the one second sampling period of the sensors. If it is necessary to terminate the estimator after one sample period, the current sub-optimal iterate of this SQP algorithm will satisfy the position constraints. Note that the first and second order extended Kalman filters also generally produced an estimate within the one second sample period while the iterative filter generally did not.

Figures 7 and 8 compare the x -direction and y -direction tracking error for the nonlinear least squares estimator and the constrained first order filter. We choose the first order filter for comparison since it generated the least noisy position estimates.

5. Results

Table 1 presents the 2-norm of the tracking errors for each estimation algorithm. The least squares estimator outperforms the extended Kalman filtering techniques by a significant margin for the x and y directions, which are the most important for source tracking. The height of the source, the z -direction, was not varied during the test. However, all four sensors were at the same height which makes it difficult to resolve the source height from the sensor measurements. For this reason, the z -direction tracking errors were not presented graphically. Figure 9 presents the change in

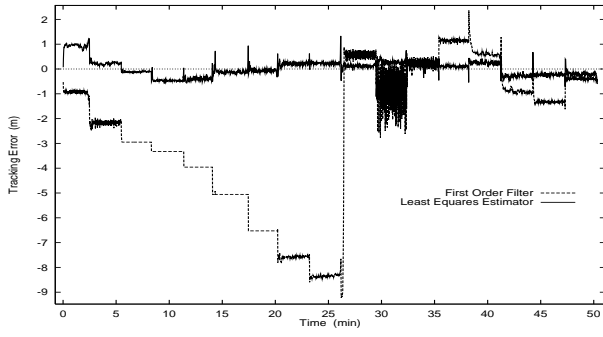


Figure 7: Constrained x -direction tracking error.

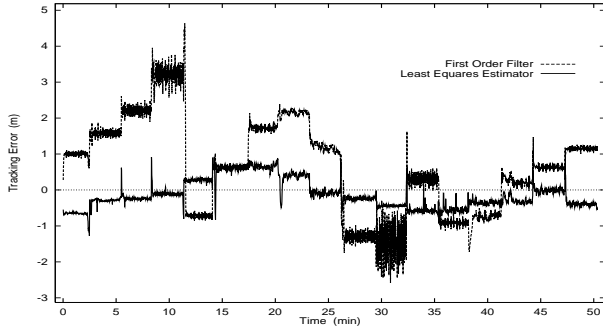


Figure 8: Constrained y -direction tracking error.

the background radiation for each of the constrained estimators. In addition to a significant position tracking error, the extended Kalman filters also estimated a much larger increase in the background radiation during the test period. Decreasing the value of α in Eq. 13 to reduce the estimated background radiation change either had little positive effect or a negative effect on the tracking errors. This study used the same dispersion and state covariance tuning parameters for each estimator. Although slight improvements with the extended Kalman filters are possible with tuning, the results presented here are representative of the obtainable tracking error performance for this system.

Estimator	x (m)	y (m)	z (m)	B (ct/sec)
First Order	216.9	69.1	25.3	1.42×10^4
First Order(c)	210.4	81.1	25.0	1.46×10^4
Iterative	120.7	74.3	80.1	1.18×10^4
Iterative(c)	223.3	80.9	52.0	1.33×10^4
Second Order	105.9	59.1	58.0	9.60×10^3
Second Order(c)	177.2	62.4	41.5	9.90×10^3
Least Squares	17.8	23.8	19.5	1.53×10^3

Table 1: Tracking error 2-norm. (c) = constrained.

6. Conclusions

The results of this study clearly show that extended Kalman filtering techniques are not appropriate for

this problem. The relationship for the solid angle subtended by the detector for a point source in Eq. 3 is not analytic at the origin. The discontinuity of the first derivative makes any truncated Taylor series a poor approximation to the nonlinear sensor model. The application of state constraints must be accomplished either by clipping the estimates or interactively adjusting the state covariance matrix. Both of these methods can lead to poor tracking performance. Finally, extended Kalman filtering techniques assume Gaussian distributions for the Taylor series model. Although Poisson distributed process can be approximated by a Gaussian distribution for large means, this approximation becomes less accurate as the count rate for a sensor decreases.

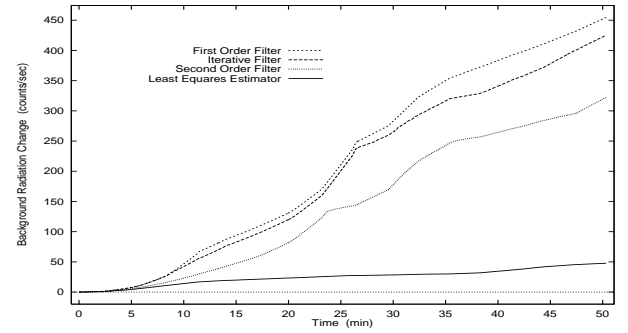


Figure 9: Estimated background radiation change.

References

- [1] N. Tsoulfanidis. *Measurement and Detection of Radiation*. McGraw-Hill, New York, 1983.
- [2] H. Gotoh and H. Yagi. Solid angle subtended by a rectangular slit. *Nuclear Instruments and Methods*, 96(2):485–486, 1971.
- [3] A. Gelb, editor. *Applied Optimal Estimation*. The M.I.T. Press, Cambridge, Massachusetts, 1974.
- [4] A. Jazwinski. *Stochastic Processes and Filter Theory*. Academic Press, New York, 1970.
- [5] M. Athans, R. Wishner, and A. Bertolini. Suboptimal state estimation for continuous-time nonlinear systems from discrete noisy measurements. *IEEE TAC*, 13(5):504–514, 1968.
- [6] J. Howse, L. Ticknor, and K. Muske. Least squares estimation techniques for position tracking of radioactive sources. *Automatica*, in press, 2001.
- [7] C. Lawrence, J. Zhou, and A. Tits. User's guide for CFSQP. Technical Report TR-94-16r1, Institute for Systems Research, University of Maryland, 1994.